

Charged-particle correlations in 600 A · MeV gold induced disassembly reactions, a statistical multifragmentation analysis

H.W. Barz ^a, W. Bauer ^b, J.P. Bondorf ^c, A.S. Botvina ^d, R. Donangelo ^e,
H. Schulz ^c, K. Sneppen ^c

^a *KAI Berlin, FZ Rossendorf, Germany*

^b *National Superconducting Cyclotron Laboratory and Department of Physics and Astronomy
Michigan State University, East Lansing, MI 48824, USA*

^c *The Niels Bohr Institute, Blegdamsvej 17, 2100 Copenhagen, Denmark*

^d *Institute for Nuclear Research, 117312 Moscow, Russia*

^e *Instituto de Física, Universidade Federal do Rio de Janeiro, 21945 Rio de Janeiro, Brazil*

Received 26 November 1992

(Revised 31 March 1993)

Abstract

The correlations between the charges emitted in the collision of 600 A · MeV Au nuclei on different targets are analysed by using a statistical multifragmentation model. Those correlations in partition space can be well reproduced by adjusting source sizes and excitation energies as a function of the total bound charge. The source sizes and excitation energies obtained are consistent with BUU calculations and from these we estimate the time at which the system reaches the break-up configuration. We suggest to measure the transverse flow energy carried by the intermediate mass fragments in order to further constrain the conditions causing the disassembly of matter.

1. Introduction

It is now a well established experimental fact that there is a regime where, depending on the target–projectile combination and incident energy, copious production of intermediate mass fragments (IMF's) with charge $Z > 2$ takes place. This break-up of nuclear matter into many fragments is an exciting field, and the mechanisms causing the fragment formation are still being extensively debated. In particular, new 4π detector systems provide data which permit to study the charged-particle correlations within the events [1–7] and to extract valuable information on the space-time evolution of the transient nuclear system before it undergoes multifragmentation.

In the present article we present an analysis of such charged-particle correlations by means of a statistical multifragmentation model. More specifically, we

analyse the data of the collision of 600 $A \cdot \text{MeV}$ Au on different target nuclei taken by the GSI group [8]. The experimentally observed correlations between charged particles are represented as a function of Z_{bound} , which is the sum of the charges of fragments with atomic numbers $Z \geq 2$. This quantity depends on the size and also on the excitation energy of the decaying projectile-spectator system, and is expected to decrease with the centrality of the collision event. It was found that several distinct charge correlations such as the average maximum charge, Z_{max} , the intermediate mass multiplicity, M_{IMF} , the ratio of largest to second largest charge, $(Z_{\text{max}} - Z_2)/(Z_{\text{max}} + Z_2)$ and the three-body asymmetry a_3 plotted as function of Z_{bound} are almost independent of the target size. This universal behaviour was interpreted as in ref. [8] as an indication that the part of the system undergoing fragmentation is equilibrated.

Since equilibration of the nuclear system prior to its multifragment disassembly is one of the key assumptions inherent in the statistical descriptions, the main goal of the present article is to find out to what extent the large body of observed charged-particle correlations reflects equilibrium properties. The results of an analysis based solely on a statistical fragmentation model would be of marginal value only, unless they are supplemented with a dynamical model allowing to estimate in an independent way source sizes and excitation energies, which are the basis for the statistical description (see also ref. [9]).

An analysis involving the same ingredients but performed with an entirely different perspective was made in ref. [8]. There, the source sizes and excitation energies were determined by considering first the Boltzmann-like description of the collision dynamics. More specifically, the projectile-spectator region undergoing fragmentation was defined as the nucleons within a sphere in coordinate space which have not yet collided. The calculated source sizes and excitation energies were then used to run a statistical multifragmentation code. In doing so, it was ignored that the presently available dynamical models do not allow for an unambiguous determination of the break-up conditions. Another attempt to analyse the data with statistical models was carried out in ref. [10]. There it was shown that the intranuclear cascade model predicts sources which cannot describe the experimental data. Therefore, in that work the sources were chosen in such a way that improved agreement with the measured IMF multiplicity could be achieved.

In the present work we apply first a statistical multifragmentation model to determine the break-up sizes and excitation energies by adjusting part of the available data. We then check that the remaining charge correlation data is correctly reproduced by the statistical-model calculations using the previously determined input source sizes and excitation energies. In a second step we utilize a dynamical Boltzmann-like approach, which is expected to provide reliable results for the evolution of the entire collision process until shortly before the multifragment decay sets in (see refs. [11,12] and refs. therein), in order to understand how the system reaches the previously determined break-up configuration. The predic-

tions of the combination of a pure statistical and a Boltzmann-like dynamical model are presented in sect. 2, where we also comment on the need for additional information on measured flow energies (see refs. [13,14]). Concluding remarks and a summary are given in sect. 3.

2. Results and discussion

We first perform a statistical multifragmentation analysis for the charge correlations obtained from the bombardment of several target nuclei with a 600 $A \cdot \text{MeV}$ Au beam [8] and afterwards discuss these results in the light of a Boltzmann-like approach. Having the results of these two approaches at our disposal we estimate in which stage of the collision the fragments may actually be formed.

2.1. Statistical multifragmentation analysis

Statistical models [15–17] disregard the dynamics of the collision and consider instead that the weights of the possible fragmentation channels are determined through the total entropy. The essential parameters of such models are the break-up volume, the size of the decaying system (mass A_0 , charge Z_0) and the excitation energy. Therefore, we adjust these parameters in order to reproduce the main features of the measured charged particle correlations.

As statistical multifragmentation model we utilized the Copenhagen version, which calculates, in a first step, the primordial fragment distribution after the prompt break-up process, and, in a second step, the evaporation during the dynamical evolution governed by the Coulomb force [18,19]. For the adjustment of mass number and excitation energy of the source we used the measured IMF multiplicity, displayed as a function of Z_{bound} in fig. 1. This IMF multiplicity has the rise and fall pattern as a function of Z_{bound} (see also ref. [5]) already predicted in ref. [20]. In our statistical model, the excitation energy needed to crack a nucleus is predicted to be of the order of 3 MeV per nucleon, while the energy needed to vaporize a nucleus into light fragments with charge $Z < 3$ is of the order of 10–12 MeV per nucleon. According to this model, the maximum number of IMF's is produced at excitation energies around 8 MeV per nucleon. This result is in agreement with the analysis of emulsion data [13], where complete events of very central collisions of 65 $A \cdot \text{MeV}$ Ar on Ag/Br point to a thermal excitation energy of 8 MeV per nucleon of the fragmenting system.

The input parameters of the statistical calculations, i.e. its size A_0 and excitation energy E^* , are determined by adjusting them so as to reproduce the mean IMF multiplicity displayed in fig. 1. They are shown in fig. 2 as a function of Z_{bound} . This plot clearly indicates that the remnant undergoing multifragmentation becomes smaller and more highly excited with increasing centrality. In fact, going

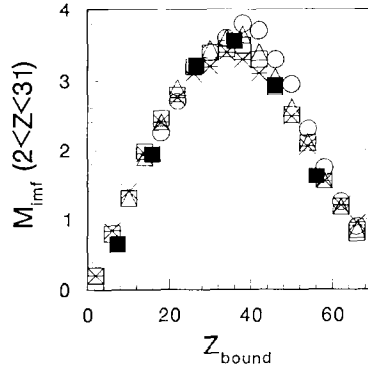


Fig. 1. The average multiplicity of IMF's for 600 $A \cdot \text{MeV}$ Au collisions on C (circles), Al (triangles), Cu (open squares) and Pb (crosses) of ref. [8], is compared with the prediction of the statistical multifragmentation model (full squares) as a function of the bound charges.

from peripheral to central collisions the excitation energy is more than doubled, whereas the remnant size decreases by an even larger factor.

We note that for the most central collisions considered the decaying remnant contains roughly 25–50 nucleons, which implies an enormous mass loss of over 70% of the Au nucleus prior to multifragmentation. Therefore, according to the statistical multifragmentation model calculations, for the most central collisions a lot of particles have to be spilled in the first violent stage of the reaction and the size of the nuclear system undergoing multifragmentation must be relatively small. Below we show that even such extreme situations can be described by a Boltzmann-like approach. Note also that for small Z_{bound} the excitation energy appears to level off at about 8 MeV per nucleon. This particular behaviour simply indicates

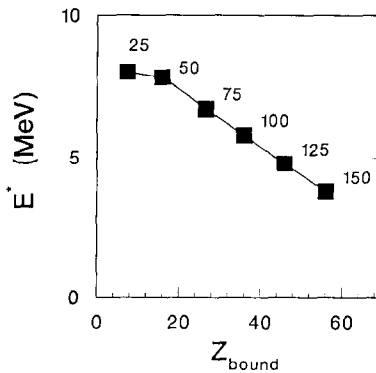


Fig. 2. The input excitation energy per nucleon E^* versus Z_{bound} used in the statistical multifragmentation model to reproduce the data of Fig. 1. The points are labelled by the mass number of the system at break-up. The line connecting them is to guide the eyes.

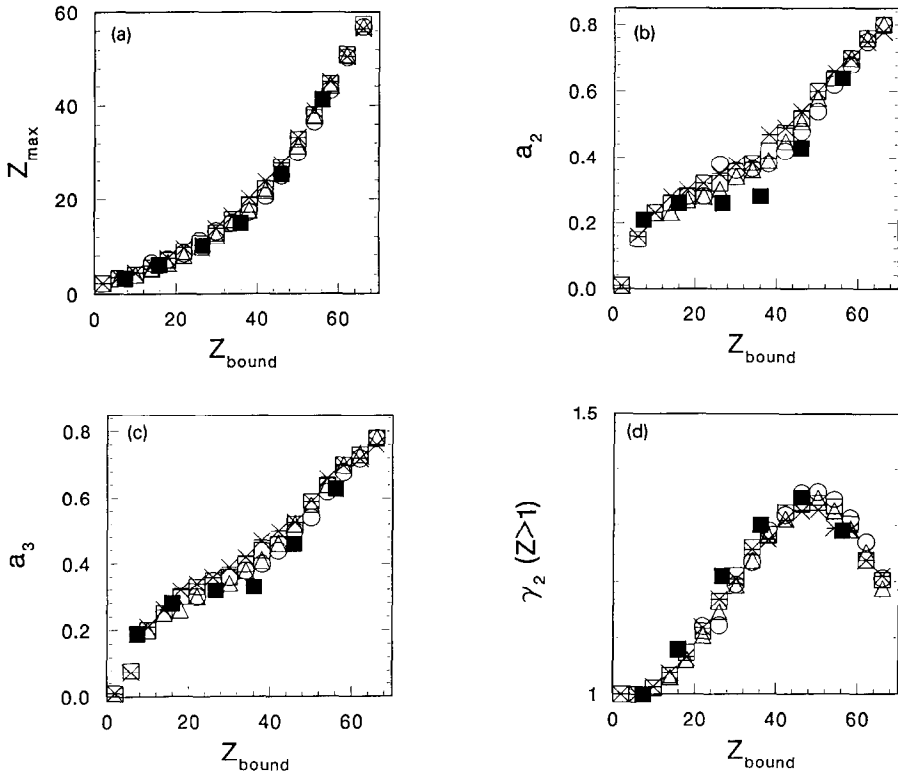


Fig. 3. (a) Same as Fig. 1 but for the average value of the maximum charge of the fragments produced in the break-up process. (b) Same as Fig. 1 but for the average value of the relative asymmetry of the two largest fragments. (c) Same as Fig. 1 but for the average value of the three-body asymmetry. (d) Same as Fig. 1 but for the average γ_2 .

that for higher excitations IMF fragments cannot be formed because the matter rapidly vaporizes through emission of unbound nucleons. Note that this limiting excitation energy for the production of IMF's is connected to the average binding energy per nucleon in finite nuclei. It is also clear from the results shown in Fig. 2 that for these high-energy collision events the main contribution to IMF production comes from the relatively cold spectator matter formed in peripheral collisions.

In order to test the predictive power of the statistical multifragmentation approach we display in Figs. 3a–3d other measured charge correlations such as the maximum charge, Z_{\max} , the ratio

$$a_2 = \frac{Z_{\max} - Z_2}{Z_{\max} + Z_2}, \quad (1)$$

where Z_2 is the second largest charge, the three-body asymmetry

$$a_3 = \frac{\sqrt{(Z_{\max} - \langle Z \rangle)^2 + (Z_2 - \langle Z \rangle)^2 + (Z_3 - \langle Z \rangle)^2}}{\sqrt{6} \langle Z \rangle} \quad (2)$$

with

$$\langle Z \rangle = \frac{1}{3}(Z_{\max} + Z_2 + Z_3) \quad (3)$$

and the γ_2 -moment [21] expressed through the variance σ_2 of the charge distribution within the event and the mean charge of the event

$$\gamma_2 = 1 + \frac{\sigma_c^2}{\langle Z \rangle_c^2}. \quad (4)$$

Together with these data we show the results of the statistical-model calculations with the same input parameters depicted in Fig. 2. A comment on the calculation of the γ_2 value is in order. If we consider only one value of the excitation energy for a given source size, the predicted value of γ_2 would be bigger than the one experimentally observed. In fact, for an infinite system near its critical point γ_2 would diverge. However, if we consider a distribution of excitation energies the value of γ_2 is decreased. In the present paper we have chosen a distribution of excitation energies that gives the observed width of the IMF distribution for a given Z_{bound} [22]. The width of the excitation-energy distribution is approximately 0.5–1.0 MeV per nucleon. We should stress that the mean values of the other charge correlations shown in Figs. 1 and 3a–3c are not sensitive to this distribution of excitation energies.

From the above comparison we learned that the statistical multifragmentation model is able to reproduce the trend of the data quite satisfactorily. This success in describing the charge correlations of the Au-induced reactions at 600 MeV per nucleon indicates that we have gained some better understanding of the source sizes and excitation energies responsible for IMF production. It becomes apparent, in particular, that the excited matter piece that undergoes multifragment decay seems to be rather small for central collisions at this high bombarding energy. In the next subsection we try to understand these results by applying a dynamical model to describe the collision process.

2.2. Dynamics prior to break-up

The Boltzmann-like treatment of the nucleus–nucleus collision process is expected to give a good estimate of the degree of thermalization in the violent stage of the collision (see refs. [11,12] and refs. therein). In this approach, nucleons are

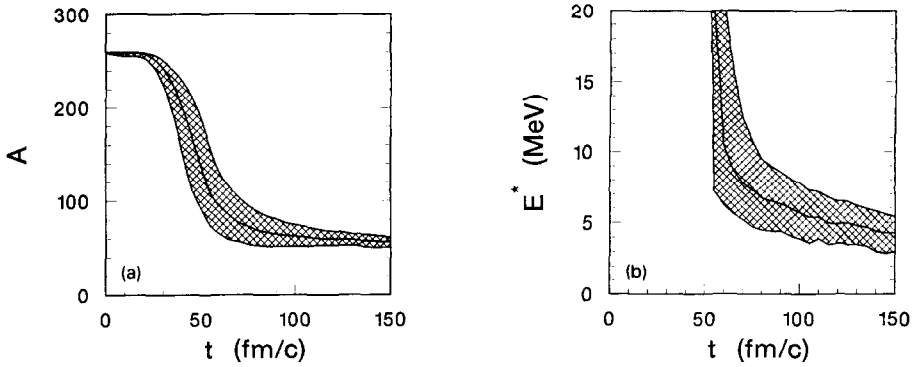


Fig. 4. (a) Remnant mass A as a function of time for three different density contours of 0.2, 0.1, and 0.05 times nuclear matter density for the lower, middle and upper curve, respectively. (b) Same as (a) but for the excitation energy per nucleon E^* .

assumed to interact with a collectively generated mean field and pairwise with each other through two-body collisions which respect the Pauli exclusion principle (see ref. [11] and refs. therein). For the subsequent calculation we utilized the Boltzmann–Uhling–Uhlenbeck (BUU) approach in the version described in detail in ref. [23]. This BUU method generates the phase-space distribution $f(\mathbf{r}, \mathbf{p}, t)$ by averaging over parallel ensembles of pseudo-nucleons.

A typical example of a BUU prediction for the collision of 600 $A \cdot \text{MeV}$ Au on Cu is illustrated in Figs. 4a–b for an impact parameter of $b = 4$ fm. In Fig. 4a we show the evolution of the mass number of nucleons inside the regions with densities higher than $\frac{1}{5}$, $\frac{1}{10}$ and $\frac{1}{20}$ of the normal nuclear matter density of $\rho_0 = 0.15 \text{ fm}^{-3}$, respectively. The results indicate clearly that in a time interval of about 30 fm/c nearly 70% of the nucleons are spilled and a remnant consisting of about 60–80 nucleons remains for a relatively long time span. In fig. 4b we display the excitation energy of the matter encircled according to the different nucleon density contours mentioned above. This excitation energy E^* was obtained by subtracting the ground-state energy of a nucleus of the same mass number and the radial-flow energy from the total energy.

Before using these results we would like to mention some additional features that emerge from the BUU calculations. First of all, let us consider the regions in the projectile-spectator in a peripheral collision ($4 < b < 8$ fm) situated closest and farthest from the participant part of the system. If we calculate the excitation energy of these two regions we find that it takes very similar values (± 0.5 MeV per nucleon) as soon as the hot participant separates from the spectator part, i.e. at times $t \geq 60$ fm/c. We can therefore conclude that the hypothesis of thermal equilibration of the fragmentating system, required by the statistical models, is well satisfied in this case.

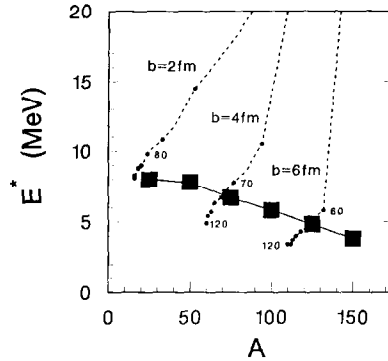


Fig. 5. Evolution of the mass number A and excitation energy E^* of the cooling remnant of the Au on Cu collision according to the BUU model for three different impact parameters (dashed lines). The dots on these lines are placed every 10 fm/c and the numbers indicate the times in fm/c. The full squares indicate the break-up conditions calculated with the statistical model already shown in Fig. 2.

Combining the results shown in Fig. 4 for the BUU approach with the results for source sizes and excitation energy inferred from the statistical multifragmentation calculation to reproduce the experimental fragmentation pattern, we see that the permissible band of excitation energies and mass numbers seems to be rather restricted. This can be seen better in Fig. 5 where are displayed the source sizes and excitation energies extracted using the statistical analysis for three different impact parameters compatible with the BUU calculations. The dots on the BUU trajectories indicate the status of the system every 10 fm/c after the beginning of the collision. For collisions at peripheral and intermediate impact parameters the disassembly process sets in at $t \geq 70$ –90 fm/c, whereas for central collisions it seems to occur considerably later. This delay in reaching the break-up configuration in central collisions is connected with the fact that considerable time is needed to spill a large number of fast nucleons before the remnant has cooled to excitations where the overall conditions allow for formation of nuclear fragments.

In ref. [8] the fragmenting projectile-spectator was defined as all nucleons within a sphere in coordinate space. Since the position and size of this sphere were taken such as to include all projectile nucleons that have yet to undergo a nucleon–nucleon collision, the resulting source sizes and the calculated excitation energies are, in particular, larger than those deduced in the present study. Therefore, the data are by far not so well described in ref. [8] as in the present work by using the same statistical multifragmentation model.

To get further information on the actual reaction mechanism leading to fragment formation, the measurement of the radial flow energy of the IMF fragments would be rather instructive. In fact, since the beam energy is converted in preequilibrium emission, radial-flow and excitation energy, and only the latter one is a direct measure of the number of IMF fragments, the determination of the flow pattern would allow us to constrain the break-up conditions even more. Thus,

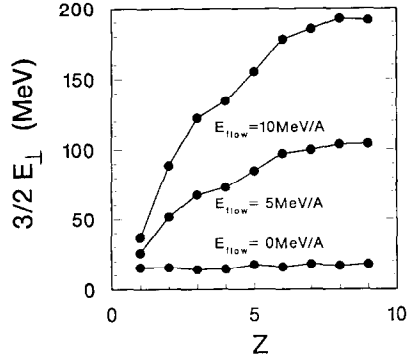


Fig. 6. Transverse kinetic energies for fragments with charge Z for three different values of the radial flow energy. The conditions studied are, according to the statistical multifragmentation model, the optimal ones for IMF production for a system of mass number $A = 100$ and excitation energy $E^* = 5.6 A \cdot \text{MeV}$.

collective flow motion present in the early stage of the collision is slowed down during the further evolution at the expense of the potential energy. Therefore, if the transverse energy of the fragments would exhibit a strong dependence on the fragment mass (charge), the fragments would necessarily have to be formed in an early stage of the collision (see also ref. [14]). For illustration we show in Fig. 6 the fragment transverse kinetic energy calculated for no radial flow, and assuming a radial flow of 5 and 10 MeV per nucleon, respectively.

The radial flow has been calculated as described in ref. [13]; i.e. the initial positions of the fragments are distributed randomly within the break-up volume with minimum possible overlap. The initial velocities have been chosen by adding the adopted radial-flow velocity to the thermal one. The system is allowed to evolve dynamically under the influence of both the mutual Coulomb repulsion between the fragments and the individual particle evaporation from the fragments. When a particle is evaporated during the expansion, its velocity and the velocity of the recoiling remnant are calculated by assuming a randomly directed emission process in the system of the decaying parent fragment.

The zero-flow calculation shown in Fig. 6 corresponds to an overall thermal equilibrium during the break-up. In this case the model predicts that the total kinetic energy becomes nearly independent of the fragments' size. This comes about because the bigger fragments tend to stay closer to the center of the evolving system and exert a smaller fraction of the Coulomb push than they would obtain on the surface of the decaying system.

One sees from Fig. 6 that the radial flow causes a nearly linear increase of the kinetic energy with the charge number. For $Z \approx 7$ this linear dependence ceases, because the finite size of the system begins to play an essential role. The centre of gravity of the big fragments cannot be near the surface of the emitting spherical source and consequently they get a smaller kinetic energy.

We think it would also be instructive to measure the longitudinal flow pattern of the IMF's to determine, for example, whether they arise from only one source as assumed here. In particular, the presence of a second source could distort the ratio of largest to second largest fragment, measured here through the charge correlation a_2 .

3. Summary

We have utilized a statistical multifragmentation model in order to describe the charge correlations obtained from the bombardment of different nuclei with a $600 A \cdot \text{MeV}$ Au beam. We found that once the source sizes and excitation energies used as input in the statistical model were adjusted so as to reproduce the dependence of the IMF multiplicity on Z_{bound} , the other measured correlations Z_{max} , $(Z_{\text{max}} - Z_2)/(Z_{\text{max}} + Z_2)$, a_3 and γ_2 were quite satisfactorily described as a function of Z_{bound} . The success of such a description provides support for the assumption that the decaying nuclear remnant is equilibrated. In the calculation of γ_2 it was necessary to consider a distribution of excitation energies, which was seen not to alter the mean values of the other correlations.

The mass number A and the excitation energy E^* extracted in order to reproduce the mean IMF multiplicity suggest that the remnant undergoing multifragmentation becomes smaller and more excited with increasing centrality. The excitation energy levels off for small Z_{bound} at 8 MeV per nucleon, suggesting that for higher excitation IMF fragment formation ceases because the matter completely vaporizes into light gaseous particles before IMF's can be formed. Collision events with impact parameters of $4 < b < 8$ fm give rise to most of the IMF's produced, because the decaying remnant is not too highly excited. Furthermore, it was found that for medium and peripheral collisions the time until disassembly sets in is of the order of 70–90 fm/ c . For central collisions it takes a significantly longer time to reach the break-up configuration, because a considerable number of highly excited nucleons is emitted before the multifragmentation takes place.

Our analysis shows that the experimental charge correlations constrain the size and excitation energy of the fragmenting residue compatible with a BUU approach and statistical multifragmentation. Since this scenario for the fragmentation of the Au nucleus relies on the assumption that even at medium impact parameters the fragmenting nuclear system is relatively small due to the enormous preequilibrium emission processes, we suggest to measure the flow energy of the fragments, in order to further constrain the conditions causing the multifragment decay.

W.B. acknowledges support from the US National Science Foundation, grant number PHY-9017077 and a Presidential Faculty Fellow award. H.W.B., A.S.B.,

R.D. and H.S. thank the Niels Bohr Institute for the kind hospitality and working atmosphere extended to them. H.W.B. acknowledges support by the German BMFT contract 06DR107. A.S.B. and R.D. thank the Niels Bohr Institute for financial support. R.D. acknowledges partial financial support from the Brazilian National Research Council (CNPq). H.S. acknowledges support from the Leon Rosenfeld Scholarship Fund. K.S. acknowledges support from the Carlsberg Foundation.

References

- [1] Y.D. Kim et al., *Phys. Rev. Lett.* 63 (1989) 494
- [2] E. Piasecki et al., *Phys. Rev. Lett.* 66 (1991) 1291
- [3] Y. Blumenfeld et al., *Phys. Rev. Lett.* 66 (1991) 576
- [4] S.J. Yennello et al., *Phys. Rev. Lett.* 66 (1991) 671
- [5] C.A. Ogilvie et al., *Phys. Rev. Lett.* 67 (1991) 1214
- [6] R.T. de Souza, *Phys. Lett.* B268 (1991) 6
- [7] D. Bowman et al., *Phys. Rev. Lett.* 67 (1991) 1527
- [8] P. Kreutz et al., GSI Preprint 92-23 (1992)
- [9] K. Sneppen and L. Vinet, *Nucl. Phys.* A480 (1988) 342
- [10] A.S. Botvina and I.N. Mishustin, *Phys. Lett.* B294 (1992) 23
- [11] G.F. Bertsch and S. Das Gupta, *Phys. Reports* 160 (1988) 189;
H. Stöcker and W. Greiner, *Phys. Reports* 137 (1986) 277;
P. Schuck et al., *Prog. Part. Nucl. Phys.* 22 (1989) 181;
W. Bauer, C.K. Gelbke and S. Pratt, *Ann. Rev. Nucl. Part. Sci.* 42 (1992) 77
- [12] P. Danielewicz and G.F. Bertsch, *Nucl. Phys.* A533 (1991) 712
- [13] H.W. Barz et al., *Nucl. Phys.* A531 (1991) 453
- [14] W. Bauer et al., to be published
- [15] S.E. Koonin and J. Randrup, *Nucl. Phys.* A356 (1981) 223
- [16] J.P. Bondorf, R. Donangelo, I.N. Mishustin, C.J. Pethick, H. Schulz and K. Sneppen, *Nucl. Phys.* A443 (1985) 321;
J.P. Bondorf, R. Donangelo, I.N. Mishustin and H. Schulz, *Nucl. Phys.* A444 (1986) 460;
H.W. Barz, J.P. Bondorf, R. Donangelo, I.N. Mishustin and H. Schulz, *Nucl. Phys.* A448 (1986) 753
- [17] Sa Ban-hao and D.H.E. Gross, *Nucl. Phys.* A437 (1985) 643;
D.H.E. Gross, Zhang Xiao-ze and Xu Shu-yan, *Phys. Rev. Lett.* 56 (1986) 1544;
X.Z. Zhang, D.H.E. Gross, S.Y. Xu and Y.M. Zheng, *Nucl. Phys.* A461 (1987) 641; A461 (1987) 668
- [18] H.W. Barz, J.P. Bondorf and H. Schulz, *Nucl. Phys.* A462 (1987) 742
- [19] H.W. Barz, J.P. Bondorf, H. Schulz and K. Sneppen, *Phys. Lett.* B244 (1990) 161
- [20] J.P. Bondorf, R. Donangelo, H. Schulz and K. Sneppen, *Phys. Lett.* B162 (1985) 30;
H.W. Barz, J.P. Bondorf and H. Schulz, *Phys. Lett.* B184 (1987) 125
- [21] X. Campi, *Phys. Lett.* B208 (1988) 351
- [22] W. Trautmann, private communication
- [23] W. Bauer et al., *Phys. Rev.* C34 (1986) 2127;
W. Bauer, *Phys. Rev. Lett.* 61 (1988) 2534